#### **CHAPTER 10**

# EFFECTS OF MODE TRUNCATION AND DISSIPATION ON PREDICTIONS OF HIGHER ORDER STATISTICS

James M. Kaihatu<sup>1</sup> and James T. Kirby, Member, ASCE<sup>2</sup>

#### Abstract

We investigate the effects mode truncation and dissipation characteristics have on predictions of wave shape statistics such as skewness and asymmetry. We demonstrate the effect of mode truncation by calculating wave shape statistics for data from a laboratory experiment using an increasing number of frequency components each calculation. We find that the values of skewness and asymmetry converge to a maximum as more components are retained, with the maximum values attained when components out to the Nyquist frequency are kept. We run a lowest order Boussinesq shoaling model and a nonlinear dispersive shoaling model with the data, retaining more components with each simulation. Both models show the same convergence characteristics as the data as the number of retained frequency components increases. The lowest order Boussinesq model, despite its shallow water formalism, yields skewness and asymmetry values closer to those of the data than those of the dispersive model. This is likely due to the phase mismatches in the dispersive model, which become large in deep water and thus violate the slowly-varying amplitude assumption. We also investigate the effect of spectral dissipation on these predictions. We run the lowest order Boussinesq shoaling model with different proportions of frequency-dependent dissipation and calculate wave shape statistics. We find that the distribution must take into account some aspect of  $(f)^2$  variation in the dissipation for reliable wave shape statistics.

#### Introduction

The Boussinesq equations (Peregrine 1967) are robust predictors of weakly nonlinear wave propagation in shallow water. The "consistent" frequency domain Boussinesq model of Freilich and Guza (1984) has been used in a number of studies (e.g., Elgar and Guza 1985; Elgar et al. 1990) concerning nearshore wave propagation; they have shown that this model does predict shallow water wave spectra reliably provided that kh << O(1), where k is the wave number and k the water depth.

Oceanographer, Oceanography Division (Code 7322), Naval Research Laboratory, Stennis Space Center, MS 39529-5004

<sup>&</sup>lt;sup>2</sup> Professor, Center for Applied Coastal Research, University of Delaware, Newark, DE 19716

In recent years, however, frequency domain models with fewer restrictions on the value of *kh* have been developed (e.g., Madsen and Sorensen 1993; Agnon et al. 1993; Kaihatu and Kirby 1995). These models, because of their dispersive nature, can be applied in greater water depths (and take into account a greater frequency range) than the lower-order Boussinesq-type models. Application of these models to laboratory data have shown their utility.

A different test of these frequency domain models would be to evaluate their ability to replicate surface shape characteristics. This involves evaluating quantities such as skewness and asymmetry. These higher order statistical quantities track the free surface characteristics of waves, and thus lend insight into the effect nonlinear energy exchange has on the evolution of the wave shape.

Elgar et al. (1990) have investigated skewness and asymmetry predictions from the consistent model of Freilich and Guza (1984) and compared these quantities to field data taken at both Torrey Pines, CA and Santa Barbara, CA in 1980. Because of the lowest order dispersion characteristics of the model, the simulations required an upper frequency cutoff that was based on the relative magnitude of the dispersion parameter kh. This upper frequency was established prior to simulation and analysis so that no nonlinear interaction with frequencies beyond the cutoff could occur. They found good data-model agreement for relatively narrow banded spectra, but somewhat poorer agreement for broad banded spectra. This is primarily due to the spectral energy content beyond the cutoff frequency for the broad spectra data.

No corresponding studies have been undertaken for the more dispersive frequency domain models, particularly as applied to field measurements. The ability of these models to simulate processes at frequencies beyond the small kh limit is particularly germane to this problem. Bowen (1994) showed that the calculation of skewness and asymmetry varied significantly with the number of harmonics of the spectral peak retained. He used his laboratory data of shoaling irregular waves on a slope to calculate these quantities with varying numbers of harmonics of the spectral peak, and found that the values of skewness and asymmetry converged to a maximum as the number of components retained increased. The maximum values of skewness and asymmetry were reached when the upper limit cutoff frequency reached the Nyquist limit. Bowen (1994) also noted that the differences between the values of skewness and asymmetry as the number of components increased were most marked in the breaking zone. This would likely be due to the increased nonlinear shifting of energy to the higher frequency components. The dependence of skewness and asymmetry on the number of retained components was not evident in the work of Elgar et al. (1990) due to the dispersion-based upper frequency cutoff for both model and data. This upper frequency cutoff is not a function of kh in the more dispersive frequency domain models, so a different criteria needs to be applied to determine this cutoff. Kaihatu and Kirby (1995), for example, use percentage of total variance. Other concerns, such as upper frequency limitations on pressure to surface conversions

(required when deducing free surface fluctuations from pressure records), can also affect the choice of cutoff frequency.

In this study we wish to investigate the effect the upper frequency cutoff has on simulating these higher order statistics. We will first investigate skewness and asymmetry values gleaned from experimental data. This will also lend insight into the sensitivity of these statistics to cutoff frequency. We will then run two shoaling models and determine the effect that retaining various numbers of components has on the reliability of predictions of skewness and asymmetry. We will find that the nature of the model has a strong effect on the predictions.

## Skewness and Asymmetry in the Wavefield

As waves in the nearshore shoal, nonlinear effects become more important. The wave crests become sharper and the crests flatter. This is represented as an increase in skewness (asymmetry about a horizonal plane). As the waves begin to approach breaking, the front face of the wave becomes steeper. This is quantified as an increase in negative asymmetry (in this context, referring to asymmetry about a vertical plane).

Skewness is defined as:

$$skewness = \frac{\left\langle \eta^3 \right\rangle}{\left\langle \eta^2 \right\rangle^{\frac{3}{2}}} \tag{1}$$

and asymmetry as:

asymmetry = 
$$\frac{\langle H(\eta^3) \rangle}{\langle \eta^2 \rangle^{\frac{3}{2}}}$$
 (2)

where the brackets denote a time average,  $\eta$  is the free surface elevation and H is the Hilbert transform.

We will be working with the Case 2 data of Mase and Kirby (1992); full details of the experimental setup can be found therein. The tank consisted of a constant depth section (h=47cm) of 10m length, and a 1:20 slope. A Pierson-Moskowitz spectrum was input at the wave paddle. For Case 2, the value of kh at the spectral peak in the deep portion of the tank was 1.9, a severe test of the dispersive wave models. In this experiment, the sampling rate  $\Delta t = 0.05s$  with the data divided into seven realizations at 2048 points each. The Nyquist frequency was 10Hz. The evolution characteristics of this data are shown in Figure 1. This figure shows the spectra at several gages taken out to the Nyquist frequency. It is apparent that the high frequency tail increases in energy, particularly in shallow water.

We use (1) and (2) to calculate the higher order statistics from the data. For each calculation we retain in turn 300, 500, 700, 900, and 1024 frequency

components (1024 components takes the calculation to the Nyquist limit). Plots of  $H_{rms}$  (root-mean-square wave height), skewness and asymmetry appear in Figure 2. There is not much difference between the measured  $H_{rms}$  values for different numbers of retained components; this implies that N=300 retains a significant percentage of the energy content in the spectrum. However, the skewness and asymmetry values clearly indicate that the number of retained frequency components has a profound effect on the calculation of high order statistics, with an increase in the number of components evidencing a convergence to a maximum value. The differences are most apparent in the nearshore, as nonlinearity becomes more prevalent in the wavefield. Additionally, the skewness measure for the N=300 case is clearly less than those for more retained components even in the offshore area, an indication that this number of components is insufficient to describe the evolution of the shape of the wavefield. This is in spite of the fact that N=300 retains sufficient energy for  $H_{rms}$  quantification.

#### **Shoaling Models**

Now that we have demonstrated the effect the number of retained components has on the evaluation of skewness and asymmetry, we now wish to determine how this affects our ability to accurately model these effects. This is more germane for the dispersive models, since the linear characteristics of the higher frequencies could be more accurately modeled

The consistent model of Freilich and Guza (1984) is:

$$A_{nx} + \frac{h_x}{4h} A_n - \frac{in^3 k^3 h^2}{6} A_n + \frac{3ink}{8h} \left( \sum_{l=1}^{n-1} A_l A_{n-l} + 2 \sum_{l=1}^{N-n} A_l^* A_{n+l} \right) = -\alpha_n A_n$$
 (3)

where A is the complex amplitude, and N is the index of the highest frequency component considered. The right hand side is a dissipation term that removes energy from the spectrum in accordance with the probabilistic dissipation expression of Thornton and Guza (1983). The distribution of that dissipation over the frequency range is discussed in a later section. The second term in (3) is the Green's Law shoaling term.

The nonlinear finite-depth shoaling model of Kaihatu and Kirby is:

$$A_{nx} + \frac{C_{gnx}}{2C_g} A_n + \frac{i}{8\omega_n C_{gn}} \left( \sum_{l=1}^{n-1} RA_l A_{n-l} e^{i\Theta} + 2 \sum_{l=1}^{N-n} SA_l^* A_{n+l} e^{i\Psi} \right) = -\alpha_n A_n$$
 (4)

where R and S are interaction coefficients, and:

$$\Theta = \int k_l + k_{n-l} - k_n dx \tag{5}$$

$$\Psi = \int k_{n+1} - k_1 - k_n dx \tag{6}$$

are referred to as "phase mismatches" since they determine the relative amount of detuning away from resonance in x. They have the capacity to become quite large in deep water, thus causing the nonlinear term to oscillate. The expansion technique used to derive (4) assumes that the amplitudes are slowly varying in space, an assumption which may be violated in deep water.

We use the shoaling models to determine the effect of the cutoff frequency on the simulation of these higher order statistics. Both models utilized error-checked variable stepsize ODE integration schemes; the consistent model used the Bulirsch-Stoer method with Richardson extrapolation, while the dispersive model used a fourth order Runge-Kutta scheme. We note that the consistent model of Freilich and Guza (1984) is formally invalid in this water depth. The lack of phase mismatch in the model is due to the nondispersive nature of the

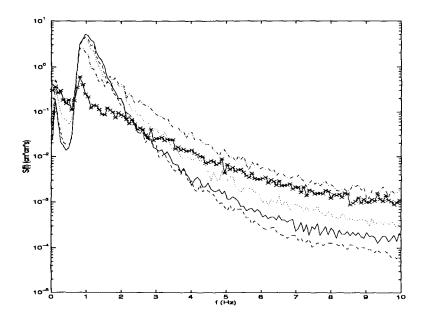


Figure 1. Evolution of spectra in experiment of Mase and Kirby (1992). Top figure: h=47cm (solid), h=25cm (dashed), h=15cm (dotted), h=7.5cm (dash-dot), h=2.5cm (dash-x)

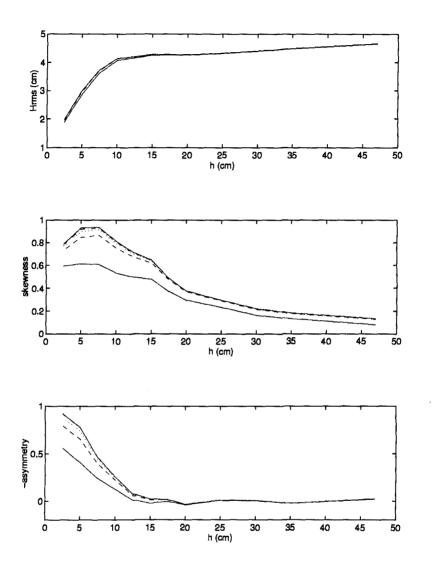


Figure 2. Statistics calculated from Case 2 data of Mase and Kirby (1992). In each figure: N=300 (bottom solid), N=500 (dashed), N=700 (dotted), N=900 (dashed), N=1024 (top solid). Top figure:  $H_{rms}$ . Middle figure: skewness. Bottom figure: - asymmetry.

nonlinear terms; in shallow water  $k_n = nk_l$ , where  $k_l$  is the wavenumber associated with the lowest frequency  $\omega_l$  in the spectrum. This causes the phase mismatches to become zero. The dispersive models, with the finite phase mismatches, have linear characteristics that work well in deep water, but have nonlinear terms that may oscillate fast enough in deep water to cause difficulty in replicating the wave shape. The phase mismatches are a consequence of the somewhat misordered derivation of the dispersive models.

We ran the two models with increasing numbers of components (N=300, 500, 700, 900 and 1024) to simulate the experiment of Mase and Kirby (1992). Then we filter the data similarly, and calculate  $H_{rms}$  and third moments. The comparisons between the consistent model and the data are shown in Figure 3. We were able to simulate the spectrum out to the Nyquist frequency with this model; it is relatively expedient compared to the more computationally intensive dispersive model (4). Even so, the consistent model with N=900 and N=1024 requires substantial computational resources. Most runs were performed on the US Army Waterways Experiment Station Cray YM-P. The N=900 and N=1024 runs, however, required a Cray batch queue with a very low assigned priority; thus these were done, one realization at a time, on a Silicon Graphics Indy.

Figure 3 shows that the consistent model greatly overpredicts the  $H_{rms}$  values of the data. This is not surprising, since the model is clearly outside its area of validity; Green's Law, the linear shoaling mechanism in the consistent model, overpredicts the shallow water spectral amplitudes when initialized in deep water. In addition, the model results for all simulations agree, which indicates that N=300 is sufficient for describing the energy level in the spectrum. The skewness and asymmetry values, on the other hand, agree reasonably well with the data. This seems inconsistent with the fact that the consistent model is far outside its range of validity. Additionally, the model results show the same tendency to converge to a maximum value as N increases as shown by the data.

The dispersive model (4) required significantly more computational resources than the consistent model. This is primarily due to the phase mismatches of the dispersive model; their size in deep water causes difficulty in solving the sets of equations. Available computational resources only allowed the N=300 and N=500 cases to be run with this model.

Figure 4 shows the comparisons between the statistics from the experiment of Mase and Kirby (1992) and the dispersive model (4). The  $H_{rms}$  comparison is not unexpected, since the dispersive model does have the ability to reliably model spectral shoaling from deep to shallow water. The third moment comparisons, however, look worse than those of the consistent model. This is somewhat surprising, since the dispersive model has linear characteristics that can be applied to deeper water. However, the likely cause of these deleterious comparisons are the phase mismatches. We define a normalized phase mismatch:

$$M = \frac{\left| k_1 - k_{N-1} - k_N \right|}{k_N} \tag{7}$$

The magnitude of M when N=1024 is 25 in the deep portion of the tank. This magnitude of mismatch can induce oscillations which have deleterious effects on the replication of the free surface. Thus, these phase mismatches serve to keep the wave from attaining a realistic form. This is not evident in spectra comparisons shown in studies of dispersive frequency domain models (e.g., Agnon et al. 1993; Kaihatu and Kirby 1995) since these effects are averaged.

One feature that is apparent with both the consistent and dispersive model simulations is that the model results underpredict the skewness and asymmetry values seen in the data for each particular cutoff frequency; this is true even at the Nyquist frequency. One reason for this underprediction for N<1024 is that all frequencies of the data have undergone nonlinear energy exchange with all others, while the model simulations are limited to those below the cutoff.

#### **Effect of Dissipation Mechanism on Statistics**

Both models have a dissipation mechanism that removes energy in the spectrum based on a probabilistic decay function developed by Thornton and Guza (1983). This dissipation mechanism is:

$$\alpha_n = \alpha_{n0} + \left(\frac{f_n}{f_{peak}}\right)^2 \alpha_{n1} \tag{8}$$

where:

$$\alpha_{n0} = F\beta(x) \tag{9}$$

$$\alpha_{n1} = \left(\beta(x) - \alpha_{n0}\right) \left( \frac{f_{peak}^2 \sum_{n=1}^{N} |A_n|^2}{\sum_{n=1}^{N} f_n^2 |A_n|^2} \right)$$
(10)

where  $f_{peak}$  is the peak frequency of the spectrum,  $f_n$  is the  $n^{th}$  frequency, F is a weighting factor, and  $\beta(x)$  is the simple dissipation model of Thornton and Guza:

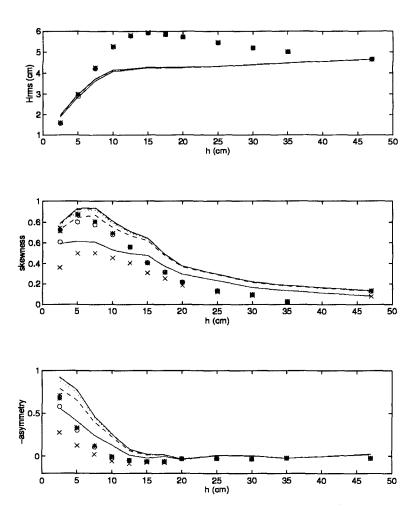


Figure 3. Comparison of modeled statistics to data of Mase and Kirby (1992) using the consistent model of Freilich and Guza (1984). In each figure: N=300 (bottom solid line is data, bottom "x" is model), N=500 (dashed line is data, "o" is model), N=700 (dotted line is data, "\*" is model), N=900 (dash-dot line is data, "+" is model), N=1024 (top solid line is data, top "x" is model). Top figure:  $H_{rms}$ . Middle figure: skewness. Bottom figure: -asymmetry.

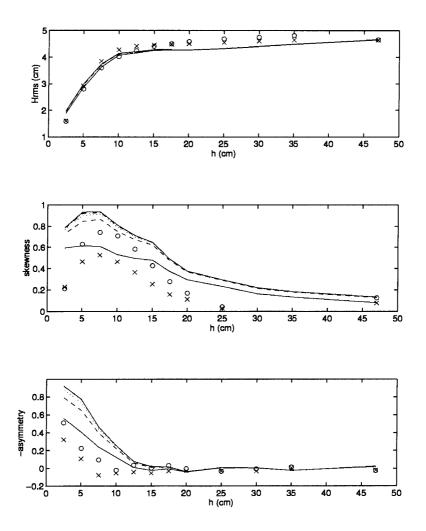


Figure 4. Comparison of modeled statistics to data of Mase and Kirby (1992) using the dispersive model of Kaihatu and Kirby (1995). In each figure: N=300 (bottom solid line is data, bottom "x" is model), N=500 (dashed line is data, "o" is model), N=700 (dotted line is data), N=900 (dash-dot line is data), N=1024 (top solid line is data). Top figure:  $H_{rms}$ . Middle figure: skewness. Bottom figure: - asymmetry.

$$\beta(x) = \frac{3\sqrt{\pi}B^{3}\bar{f}H_{rms}^{5}}{4\sqrt{gh\gamma}^{4}h^{5}}$$
(11)

where B and  $\gamma$  are free parameters set to 1.0 and 0.6, respectively. The mean frequency  $\bar{f}$  is taken to be the peak frequency. These values are close to those found by Thornton and Guza (1983). The proper value of F is a matter of some discussion; this weighing factor determines the dependence of the dissipation on frequency. Setting F=1.0 causes the dissipation to be equal across all frequencies, while setting F=0 weights the dissipation proportionally to  $(f)^2$ . Physical arguments for the proper value of F are presented elsewhere (Eldeberky and Battjes 1996; Kirby and Kaihatu 1996) and thus will not be presented here. The primary intent in this section is to discern the effect the particular value of F has on higher order statistics.

Realizing that we will not obtain accurate predictions of these quantities (for the reasons described earlier), we instead look for the effect various values of F have on the trends of the skewness and asymmetry values as waves propagate into shallow water. We ran both the consistent model of Freilich and Guza (1984) for various values of F, using N=300. Figure 5 shows skewness and asymmetry results for the consistent model with F=0, 0.25, 0.5, 0.75, and 1.0. The skewness results indicate that F=0.75 follows the trend of the data best, while the asymmetry results show that F=0.5 is most representative. However, what is more instructive are the comparisons between the simulations. The skewness values for F=0, F=0.25 and F=0.5 show a decrease at the last three gages. These values of F weight the dissipation higher towards higher frequencies, thus suppressing the nonlinear energy transfer to higher frequencies. The converse trend is evident in the asymmetry predictions. The F=0 has the most negative asymmetry for water depths up to 7.5cm, at which point the negative asymmetry unexpectedly decreases in the inner surfzone. The fact that the F=0 curve exhibits the most negative asymmetry until its sudden downturn is indicative of the sawtooth shape of the breaking waves, which are in line with an (f)<sup>2</sup> distribution of dissipation. Kirby and Kaihatu (1996) discuss the physical basis behind this supposition. As mentioned before, the F=0.5 best matches the trend of the data for the entire range of water depths. The fact that the F=1.0 curves are not the best representations of the skewness and asymmetry trends indicates that some weighting of the dissipation toward higher frequencies is required to simulate this reliably, contrary to Eldeberky and Battjes (1996), who indicate that no such weighting need take place. In fact, it may be that if all components of the spectrum out to the Nyquist frequency were retained we can rely solely on the  $(f)^2$  representation of the dissipation distribution, and that retention of  $\alpha_{n0}$  in (8) is an artifact of the truncation of the spectrum below the Nyquist frequency. Additionally, the sudden downturn of both skewness and asymmetry from the model results in the inner surf zone may also be an artifact of the mode truncation; Kirby and Kaihatu

(1996) show a comparison of third moments between the Case 2 data of Mase and Kirby (1992) and the time-domain extended Boussinesq code of Wei et al. (1995). This comparison, which utilized the entire unfiltered data set in the model simulation, showed that the time-domain model can reliably replicate third moment statistics.

#### **Conclusions**

We used the data of Mase and Kirby (1992) and two nonlinear shoaling models to investigate the effect mode truncation and dissipation mechanisms have on the prediction of third order statistics. We found that the number of components used in the calculation has a strong effect on the skewness and asymmetry values; this was true for both the data and the model simulations. The consistent model of Freilich and Guza (1984), though formally invalid for the peak kh values of the experiment, actually modeled the third order moments better than the dispersive model of Kaihatu and Kirby (1995). This is due to the phase mismatches in the dispersive model; their size in deep water causes the nonlinear term to oscillate considerably, keeping the wave from attaining a realistic form. We also looked at the effect different weightings of frequency dependent dissipation mechanisms have on the predictions of these statistics, and found that these mechanisms must contain some frequency dependence to model skewness and asymmetry realistically. This is contrary to Eldeberky and Battjes (1996), who maintained that a constant distribution of dissipation over frequency is optimum. Further work in this area will focus on continued development of the dissipation models.

### **Acknowledgments**

The first author was supported by the Office of Naval Research through the Naval Research Laboratory and a JOI/Core Post-Doctoral Fellowship. Computer time on the CEWES Cray YM-P was provided by the DoD High Performance Computing Center. The second author was supported by the Army Research Office, Grant DAAL 03-92-G-0116. This paper, NRL contribution PP/7322--96-0035, is approved for public release; distribution unlimited.

### <u>References</u>

Agnon, Y., Sheremet, A., Gonsalves, J., and Stiassnie, M., "Nonlinear evolution of a unidirectional shoaling wave field," *Coastal Engineering*, 20, pp 29-58, 1993.

Bowen, G., "Shoaling and breaking random waves on a 1:35 laboratory beach," M.S. Thesis, Civil Engineering Dept., University of Delaware, Newark, DE, 94p., 1994.

Eldeberky, Y., and Battjes, J., "Spectral modelling of wave breaking: application to Boussinesq equations," *Journal of Geophysical Research*, vol. 101, no. C1, pp. 1253-1264, 1996.

Elgar, S., and Guza, R., "Shoaling gravity waves: comparisons between field observations, linear theory, and a nonlinear model," *Journal of Fluid Mechanics*, vol. 158, pp. 47-70, 1985.

Elgar, S., Freilich, M., and Guza, R., "Model-data comparisons of moments of nonbreaking shoaling surface gravity waves," *Journal of Geophysical Research*, vol. 95, no. C9, pp. 16055-16063, 1990.

Freilich, M., and Guza, R., "Nonlinear effects on shoaling surface gravity waves," *Proceedings of the Royal Society of London*, A311, pp. 1-41, 1984.

Kaihatu, J., and Kirby, J., "Nonlinear transformation of waves in finite water depth," *Physics of Fluids*, vol. 7, no. 8, pp. 1903-1914, 1995.

Kirby, J., and Kaihatu, J., "Structure of frequency domain models for random wave breaking," *Proceedings of the 25<sup>th</sup> International Conference on Coastal Engineering*, Orlando, FL, to appear, 1996.

Madsen, P., and Sorensen, O., "Bound waves and triad interactions in shallow water," *Ocean Engineering*, vol. 18, pp. 183-204, 1993.

Mase, H., and Kirby, J., "Hybrid frequency-domain KdV equation for random wave transformation," *Proceedings of the 23<sup>rd</sup> International Conference on Coastal Engineering*, Venice, Italy, pp. 474-487, 1992.

Thornton, E., and Guza, R., "Transformation of wave height distribution," *Journal of Geophysical Research*, vol. 88, no. C10, pp. 5925-5938, 1983.

Wei, G., Kirby, J.T., Grilli, S.T., and Subramanya, R., "A fully nonlinear Boussinesq model for surface waves. Part 1. Highly nonlinear steady waves," *Journal of Fluid Mechanics*, vol. 294, pp. 71-92, 1995.

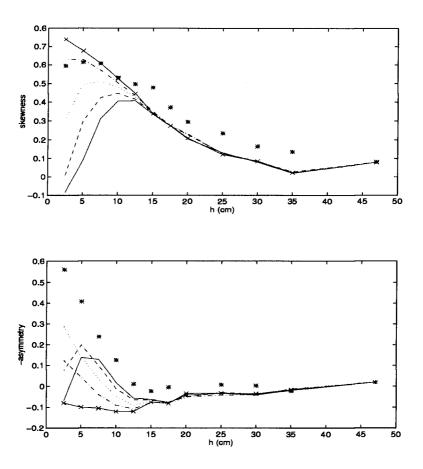


Figure 5. Skewness and asymmetry comparisons between the consistent model of Freilich and Guza (1984) and Case 2 data of Mase and Kirby (1992) for different values of F. In each figure: data (\*); F=0 (solid); F=0.25 (dashed); F=0.5 (dotted); F=0.75 (dash-dot), F=1.0 (dash-x). Top figure: skewness. Bottom figure: - asymmetry.